measurements for glaucoma detection using optical coherence tomography. Am J Ophthalmol 139:44-55.

Miyamoto-Sato E, Ishizaka M, Horisawa K, Tateyama S, Takashima H, Fuse S, Sue K, Hirai N, Masuoka K, Yanagawa H (2005) Cell-free cotranslation and selection using in vitro virus for high-throughput analysis of protein-protein interactions and complexes. Genome Res 15:710-717.

Monemi S, Spaeth G, DaSilva A, Popinchalk S, Ilitchev E, Liebmann J, Ritch R, Heon E, Crick RP, Child A, Sarfarazi M (2005) Identification of a novel adult-onset primary open-angle glaucoma (POAG) gene on 5q22.1. Hum Mol Genet 14:725-733.

Moreland RJ, Dresser ME, Rodgers JS, Roe BA, Conaway JW, Conaway RC, Hanas JS (2000) Identification of a transcription factor IIIA-interacting protein. Nucleic Acids Res 28:1986-1993.

Moritz OL, Tam BM, Hurd LL, Peranen J, Deretic D, Papermaster DS (2001) Mutant rab8 Impairs docking and fusion of rhodopsin-bearing post-Golgi membranes and causes cell death of transgenic Xenopus rods. Mol Biol Cell 12:2341-2351.

Nachury MV, Loktev AV, Zhang Q, Westlake CJ, Peränen J, Merdes A, Slusarski DC, Scheller RH, Bazan JF, Sheffield VC, Jackson PK (2007) A core complex of BBS proteins cooperates with the GTPase Rab8 to promote ciliary membrane biogenesis. Cell 129:1201-13.

Park BC, Shen X, Samaraweera M, Yue BY (2006) Studies of optineurin, a glaucoma gene: Golgi fragmentation and cell death from overexpression of wild-type and mutant optineurin in two ocular cell types. Am J Pathol 169:1976-89.

Quigley HA (1996) Number of people with glaucoma worldwide. Br J Ophthalmol 80:389-393.

Quigley HA, Broman AT (2006) The number of people with glaucoma worldwide in 2010 and 2020. Br J Ophthalmol 90:262-267.

Rangaswamy NV, Shirato S, Kaneko M, Digby BI, Robson JG, Frishman LJ (2007) Effects of Spectral Characteristics of Ganzfeld Stimuli on the Photopic Negative Response (PhNR) of the ERG. Invest Ophthalmol Vis Sci 48:4818-28.

Rezaie T, Child A, Hitchings R, Brice G, Miller L, Coca-Prados M, Heon E, Krupin T, Ritch R, Kreutzer D, Crick RP, Sarfarazi M (2002) Adult-onset primary open-angle glaucoma caused by mutations in optineurin. Science 295:1077-1079.

Sahlender DA, Roberts RC, Arden SD, Spudich G, Taylor MJ, Luzio JP, Kendrick-Jones J, Buss F (2005) Optineurin links myosin VI to the Golgi complex and is involved in Golgi organization and exocytosis. J Cell Biol 169:285-95.

Sarfarazi M, Rezaie T (2003) Optineurin in primary open angle glaucoma. Ophthalmol Clin North Am 16:529-541.

Sato T, Mushiake S, Kato Y, Sato K, Sato M, Takeda N, Ozono K, Miki K, Kubo Y, Tsuji A, Harada R, Harada A (2007) The Rab8 GTPase regulates apical protein localization in intestinal cells. Nature 448:366-9.

Senatorov V, Malyukova I, Fariss R, Wawrousek EF, Swaminathan S, Sharan SK, Tomarev S (2006) Expression of mutated mouse myocilin induces open-angle glaucoma in transgenic mice. J Neurosci 2006 26:11903-14.

Stoilov I, Akarsu AN, Sarfarazi M (1997) Identification of three different truncating mutations in cytochrome P4501B1 (CYP1B1) as the principal cause of primary congenital glaucoma (Buphthalmos) in families linked to the GLC3A locus on chromosome 2p21. Hum Mol Genet 6:641-7.

Stone EM, Fingert JH, Alward WL, Nguyen TD, Polansky JR, Sunden SL, Nishimura D, Clark AF, Nystuen A, Nichols BE, Mackey DA, Ritch R, Kalenak JW, Craven ER, Sheffield VC (1997) Identification of a gene that causes primary open angle glaucoma. Science 275:668-70.

Tan O, Li G, Lu AT, Varma R, Huang D; Advanced Imaging for Glaucoma Study Group (2008) Mapping of macular substructures with optical coherence tomography for glaucoma diagnosis. Ophthalmology 115:949-56.

Wang L, Cioffi GA, Cull G, Dong J, Fortune B (2002) Immunohistologic evidence for retinal glial cell changes in human glaucoma. Invest Ophthalmol Vis Sci 43:1088-94.

Wässle H, Grünert U, Röhrenbeck J, Boycott BB (1989) Cortical magnification factor and the ganglion cell density of the primate retina. Nature 341:643-6.

Watanabe T, Raff MC (1988) Retinal astrocytes are immigrants from the optic nerve. Nature 332:834-7.

Willoughby CE, Chan LL, Herd S, Billingsley G, Noordeh N, Levin AV, Buys Y, Trope G, Sarfarazi M, Heon E (2004) Defining the pathogenicity of optineurin in juvenile open-angle glaucoma. Invest Ophthalmol Vis Sci 45:3122-3130.

Zerial M, McBride H (2001) Rab proteins as membrane organizers. Nat Rev Mol Cell Biol 2:107-117.

FIGURE LEGENDS

Figure 1.

Development of transgenic mouse over expressing OPTN.

A, Schematic diagram of the OPTN constructs used in this study. The green region corresponds to the OPTN protein. Positions of mutations and deletions are shown in red. The HA tag is marked by yellow color. The CAGGS region corresponds to the

chicken beta-actin promoter. ***B,*** Fundus photographs of normal, Wt and E50K Tg mouse eyes at 16 month. Curvature of the retinal vessels indicates the excavation of the area including the optic disc in E50K Tg mouse eye. ***C,*** Total expression of endogenous and mutant OPTN (red) in the retina of normal and E50K Tg mice at 16 month. Anti-OPTN antibody and Anti-HA antibody were used to detect endogenous and mutant OPTN respectively. Scale bar, 50 μm.

Figure 2.

RGC loss and thinning of the retina thickness in the peripheral retina.

A, staining of retina sections of 16 month old normal and Tg mice. Scale bar, 200 μm (upper panel), 50 μm (lower panel). ***B,*** Quantification of the RGC number and retina thickness of 16 month old normal and Tg mice (n=6). Only 50K Tg mice at 16 months showed significant RGC loss and thinning of retina (**p<0.01).**C,** Quantification of the RGC number and retina thickness during development of E50K Tg mice(n=6). Tg mice showed statistically significant RGC loss and thinning of the retina starting from 12 months of age. **D,** Impaired ERG in E50K Tg mice. The amplitude of the PhNR by E50K Tg mice decreased and removed the negative wave to the transient b-wave (arrow), suggesting RGC loss and other abnormality.

Figure 3.

Histopathology of retina and optic nerve of 16 month old Wt and E50K Tg mouse eyes.

A, Immunolabeling of the retina sections with calretinin, a specific marker for RGCs and amacrine cells. Synapse disruption was observed in the E50K Tg mouse retina (arrow). Scale bar, 20 μm. ***B,*** Hematoxylin-eosin staining and immunostaining with antibodies against tubulin ß III isoform in the optic nerve region. Significant thinning of the nerve fiber layer and the excavation of optic disc (arrow) was observed in E50K Tg mice. Scale bar, 100 μm.

Figure 4.

RGC degeneration in E50K Tg mice.

A, Immunostaining of normal, Wt, and E50K Tg mouse whole retinas with antibodies against SMI32, a specific marker of large type RGCs. Scale bar, 500 μm. White box indicate the location of photographs in lane B. **B,** Thinning of NFL, RGC loss. Scale bar, 50 μm. **C,** RGC axon abnormality (arrows) was also observed. Scale bar, 50 μm.

Figure 5.

Glia cells death in E50K Tg mice.

A, B, Flat mount retina of *E50K* Tg mice was double immunostained with SMI32 (red) and active caspase-3 (green) antibodies. Apoptotic cells were observed only in the whole mount retina of E50K Tg mice. Scale bar, 100 μm. **C-E,** Flat mount retina of E50K Tg mice was also double immunostained with active caspase-3 (green) and GFAP (red) antibodies showing apoptosis of astrocytes. Scale bar, 50 μm. **F,** Apoptotic astrocytes (green) in peripheral retina. **G,** Apoptotic astrocytes (green) in central retina. Scale bar, 100 μm.

Figure 6

IOP measurements for Wt and E50K Tg mice.

A, impact-rebound tonometer and ***B,*** optical interferometry tonometer. Both methods gave normal IOP of 15 +/-1 mmHg for Tg mice at all ages examined (n=6).

Figure 7

Disruption of OPTN-Rab8 interaction by E50K mutation.

A, A diagram of cDNA constructs used in experiments to study protein-protein interaction. ***B,*** The protein-protein interaction of OPTN Wt and E50K with Rab8 Wt, T22N inactive form, and Q67L active form as measured in RGC-5 cells. Interaction of OPTN Wt and Q67L active form of Rab8 increased two and five times over Rab8 Wt

or T22N inactive form of Rab8 protein, respectively (**$p<0.01$). OPTN E50K did not show any interaction with any construct including the active form of Rab8 (n=6). ***C,*** Protein interaction of Wt or mutant OPTN E50K with Rab8 was measured by QCM technique. A sharp drop of QCM frequency was observed when control OPTN Wt was injected as guest sample, confirming the previous reports of OPTN-Rab8 interaction. Mutant OPTN E50K showed no interaction with Rab8. ***D,*** GST Pull-down assay to determine OPTN E50K-Rab8 interaction. The fusion protein GST-Rab8 was used for *in vitro* binding assay with purified OPTN Wt and OPTN E50K protein. For negative control OPTN Wt and OPTN E50K were reacted with GST alone (lane 1 & 2). *In vitro* translated OPTN Wt and OPTN E50K were analyzed by SDS-PAGE to show the protein size (lane 6 & 7). OPTN E50K showed significant loss of interaction with Rab8 compare with OPTN Wt (lane 3 & 4, graph). The illustration shows a diagram of the interaction experiment. ***E,*** Immunostaining the OPTN-Rab8 complex (green) with Golgi marker GM130 (red), indicate that these interactions take place adjacent to the Golgi network.

Figure 8.

NTG patient with OPTN E50K mutation.

A, A pedigree of a NTG family with OPTN E50K mutation. The patients were diagnosed as NTG with glaucomatous optic neuropathy and visual field loss. ***B,*** Optical coherence tomography (Cirrus HD-OCT, Carl Zeiss Meditec, Dublin , CA) and visual field test (Humphrey Field Analyzer, Carl Zeiss Medic, Dublin, CA) were shown on patient 2 and unrelated normal control. The retinal NFL thinning and glaucomatous visual field loss were observed in patients.

A

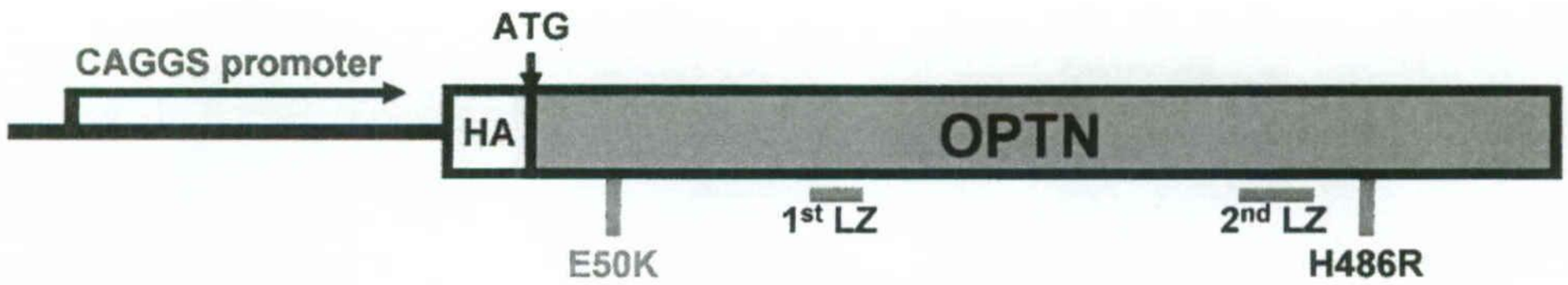
ATG
CAGGS promoter
HA
OPTN
1st LZ
2nd LZ
E50K
H486R

B

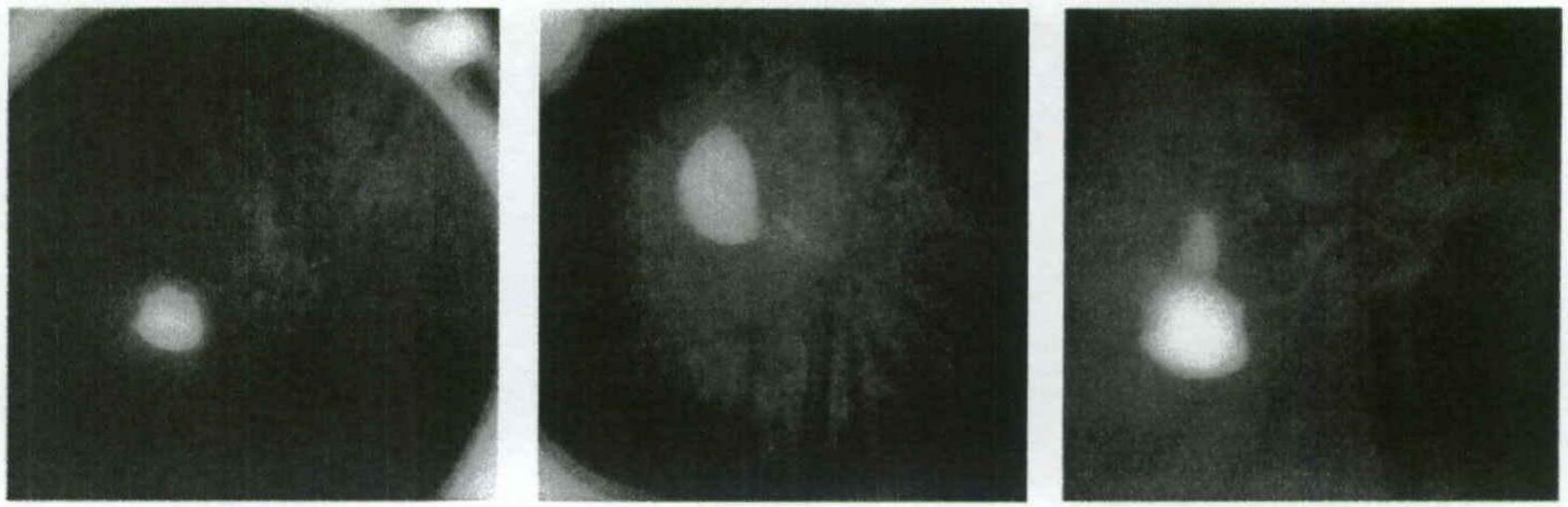

C

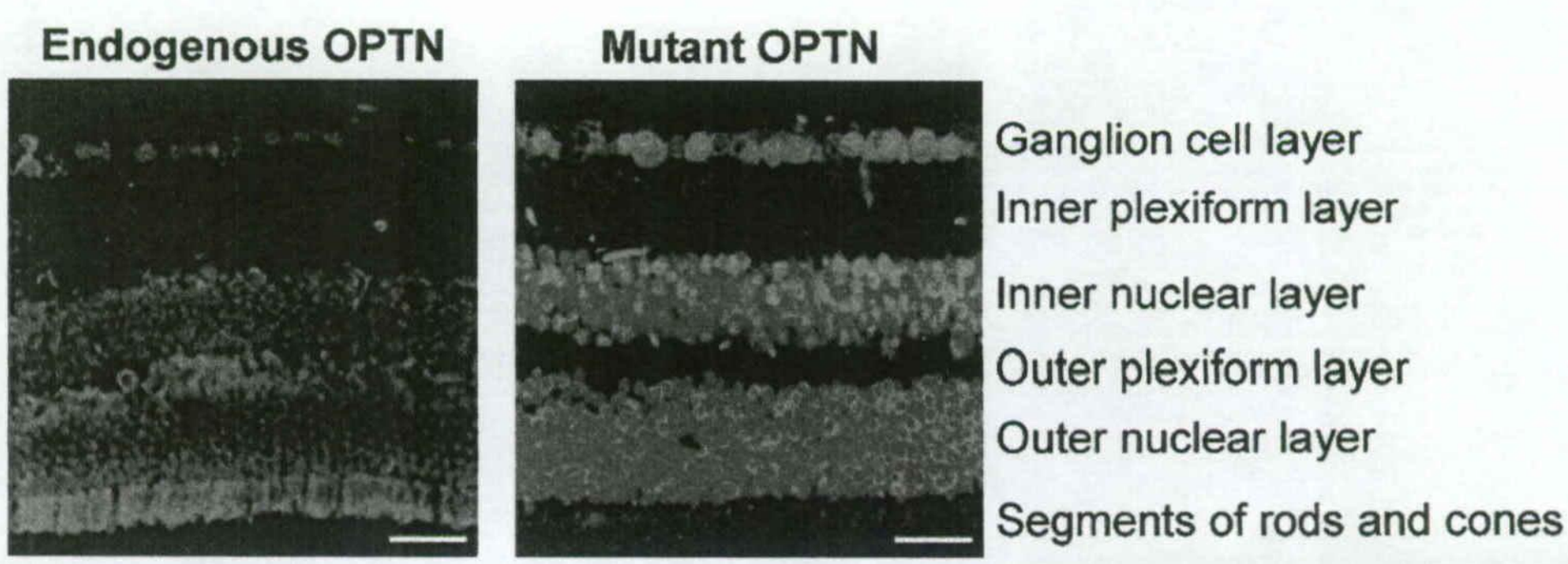
Endogenous OPTN
Mutant OPTN
Ganglion cell layer
Inner plexiform layer
Inner nuclear layer
Outer plexiform layer
Outer nuclear layer
Segments of rods and cones

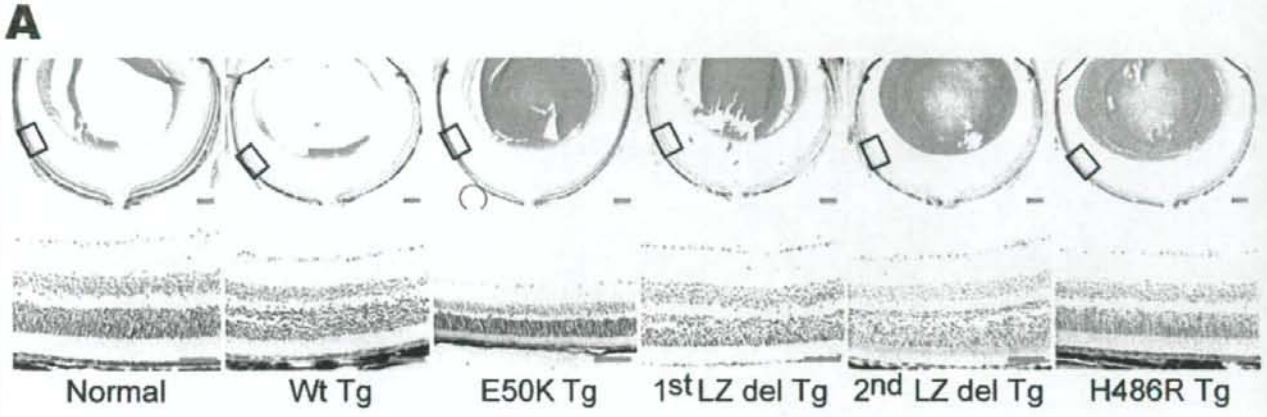
A
Normal
Wt Tg
E50K Tg
1st LZ del Tg
2nd LZ del Tg
H486R Tg

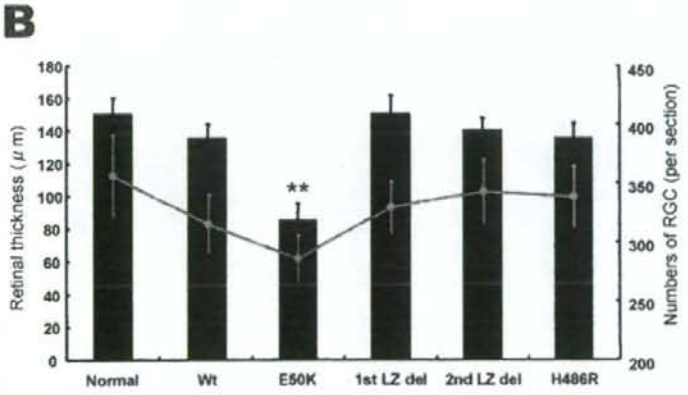
B
Retinal thickness (μm)
Numbers of RGC (per section)
**
Normal
Wt
E50K
1st LZ del
2nd LZ del
H486R

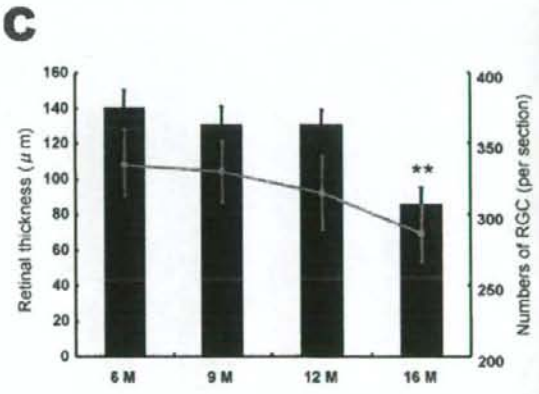
C
Retinal thickness (μm)
Numbers of RGC (per section)
**
6 M
9 M
12 M
16 M

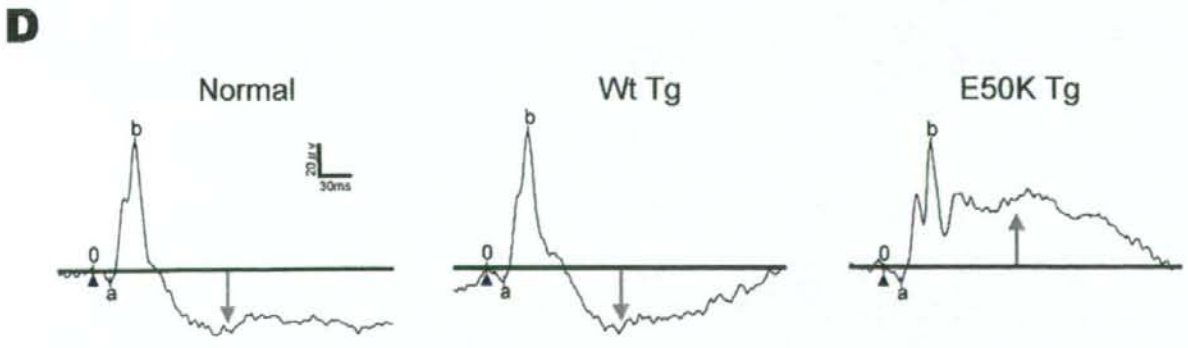
D
Normal
Wt Tg
E50K Tg
20μV
30ms
b
0
a

A

Wt Tg

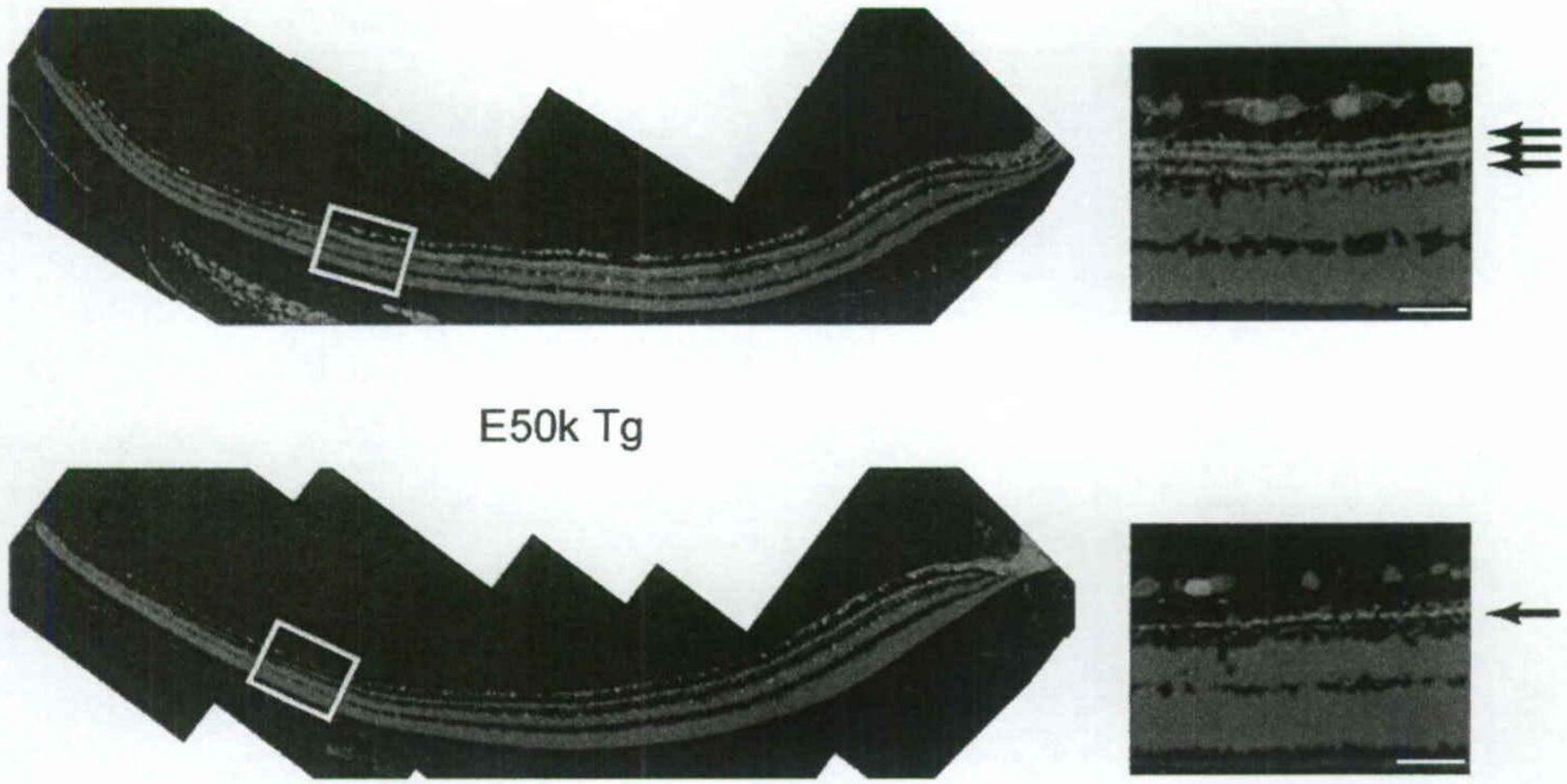

E50k Tg

B

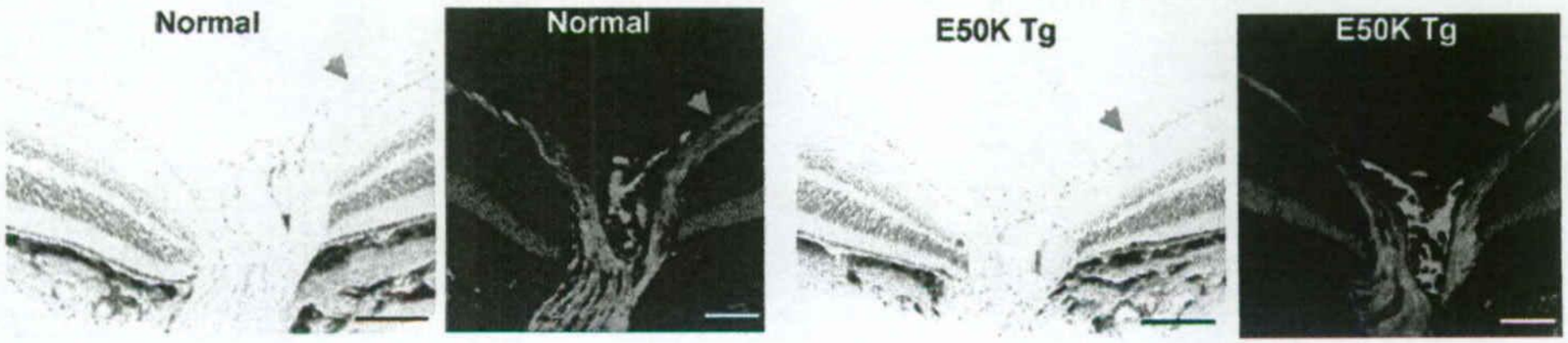

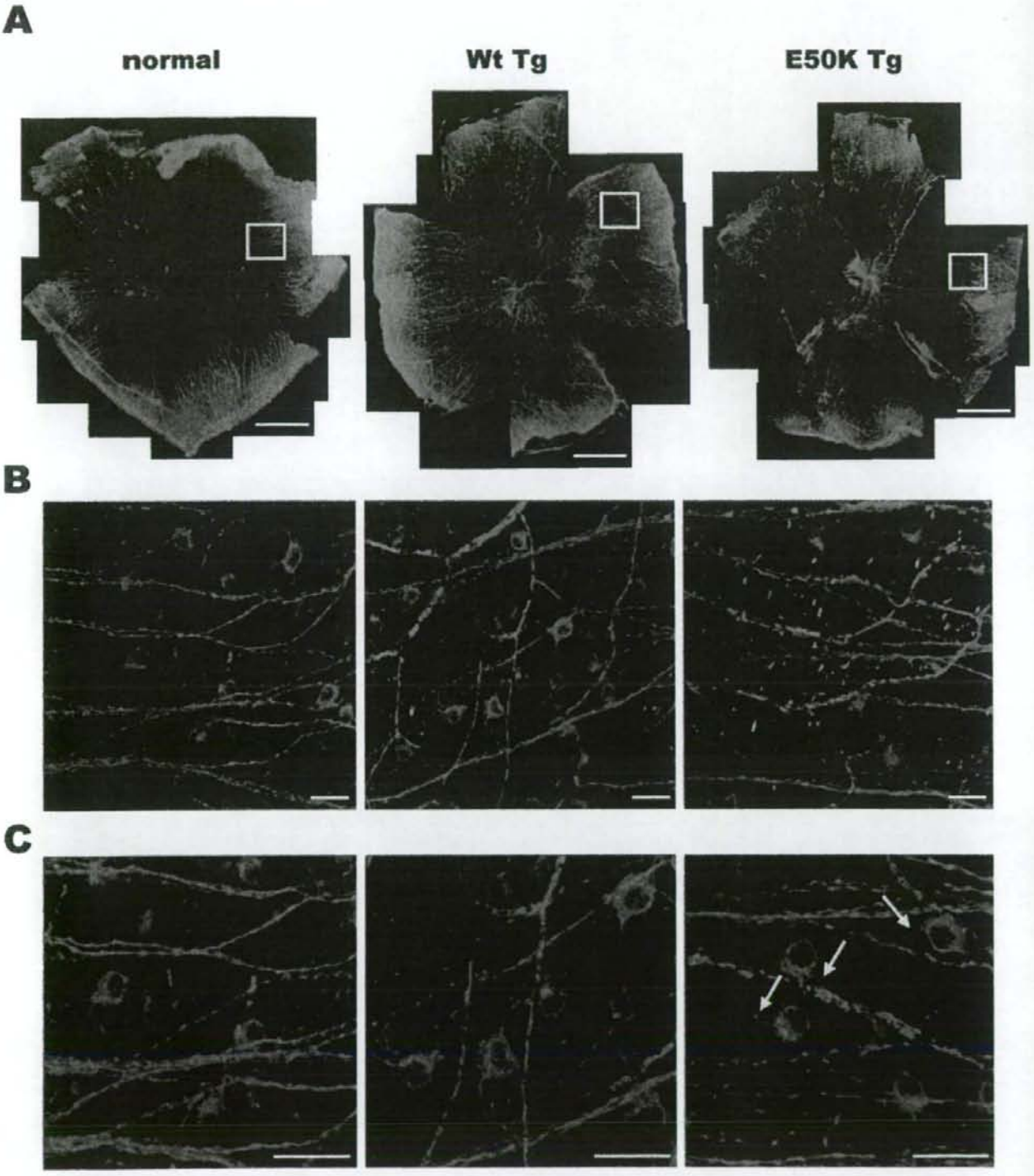
A
normal
Wt Tg
E50K Tg
B
C

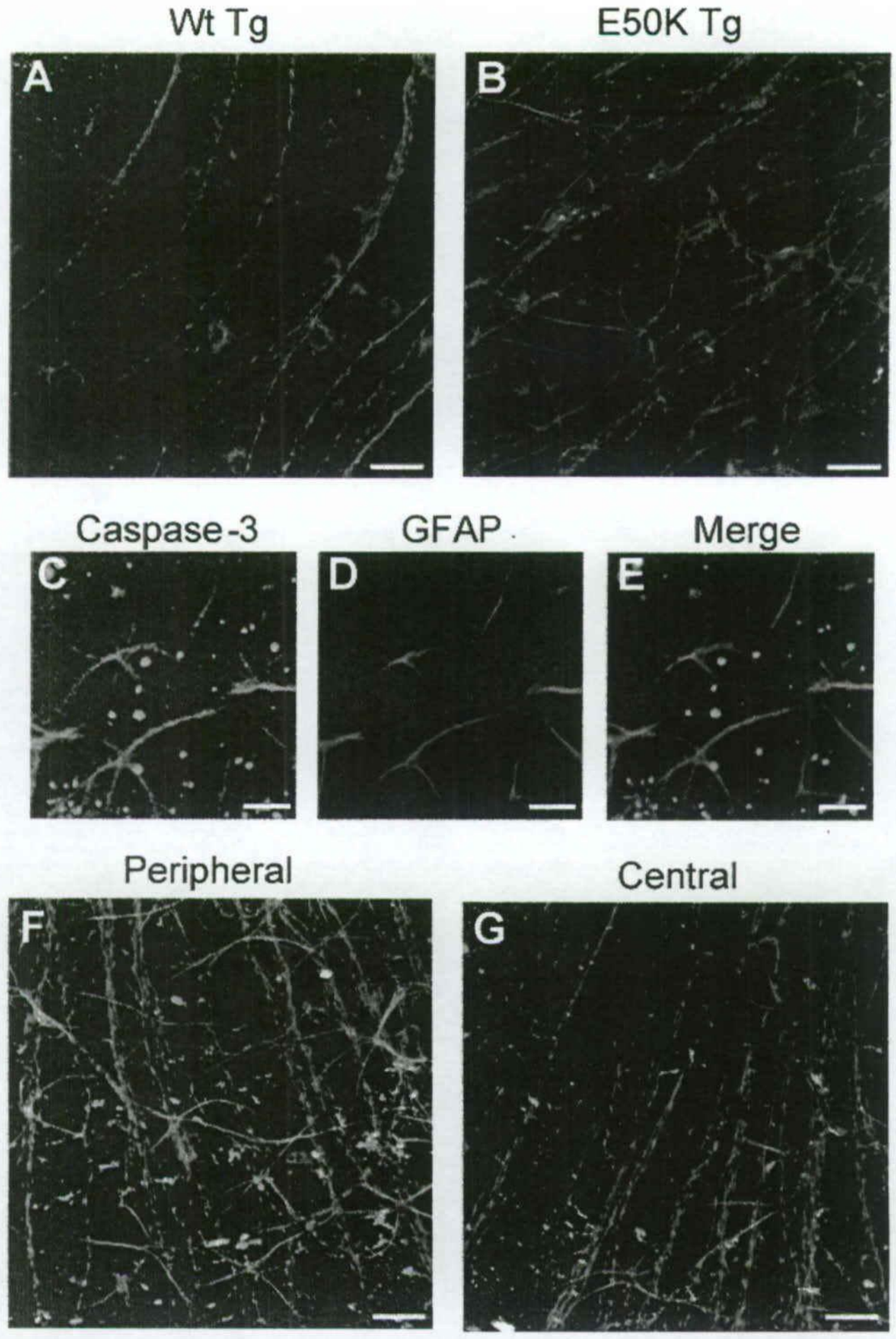
Wt Tg
E50K Tg
A
B
Caspase-3
GFAP
Merge
C
D
E
Peripheral
Central
F
G

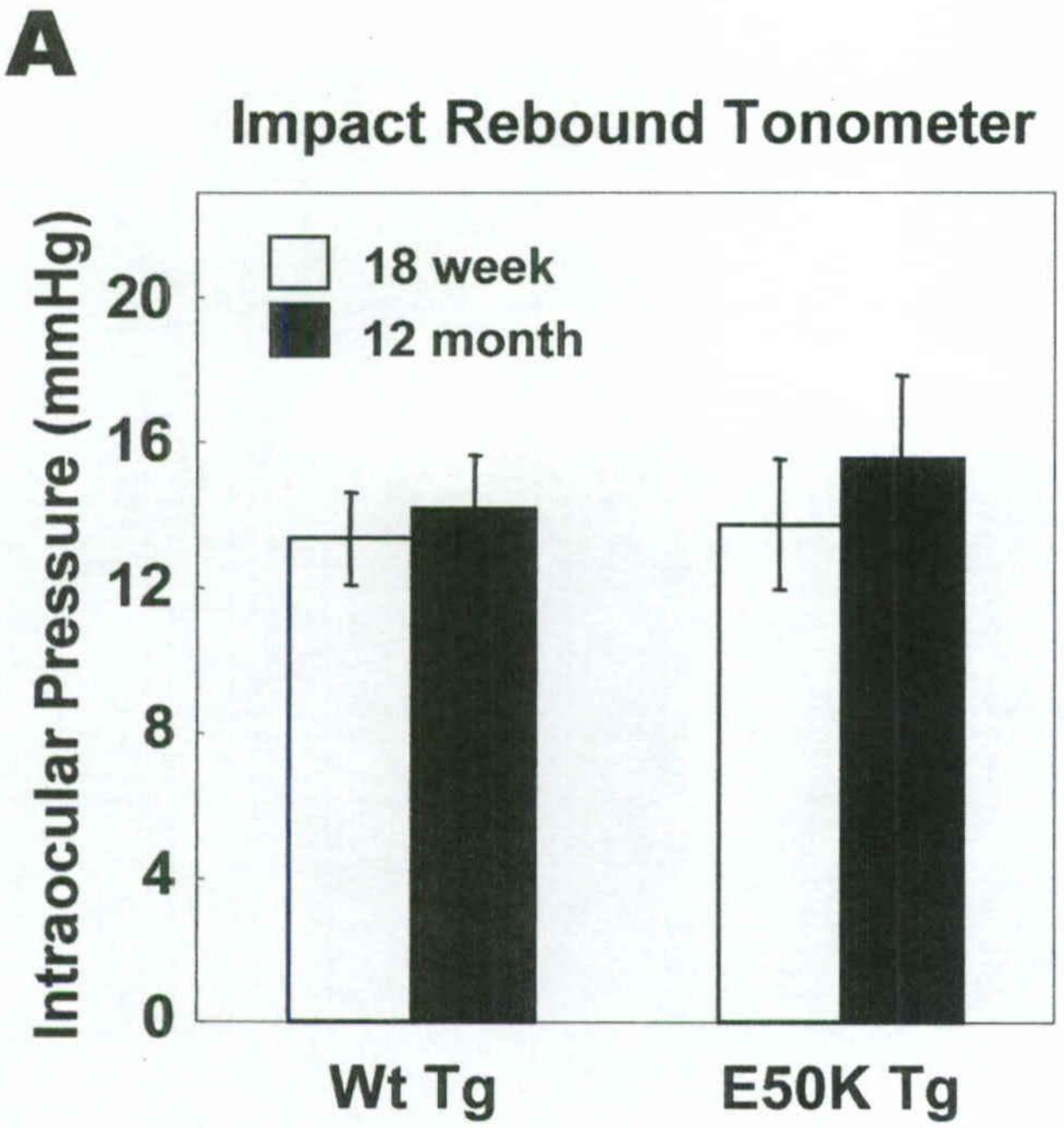
A
Impact Rebound Tonometer
18 week
12 month
Intraocular Pressure (mmHg)
0
4
8
12
16
20
Wt Tg
E50K Tg

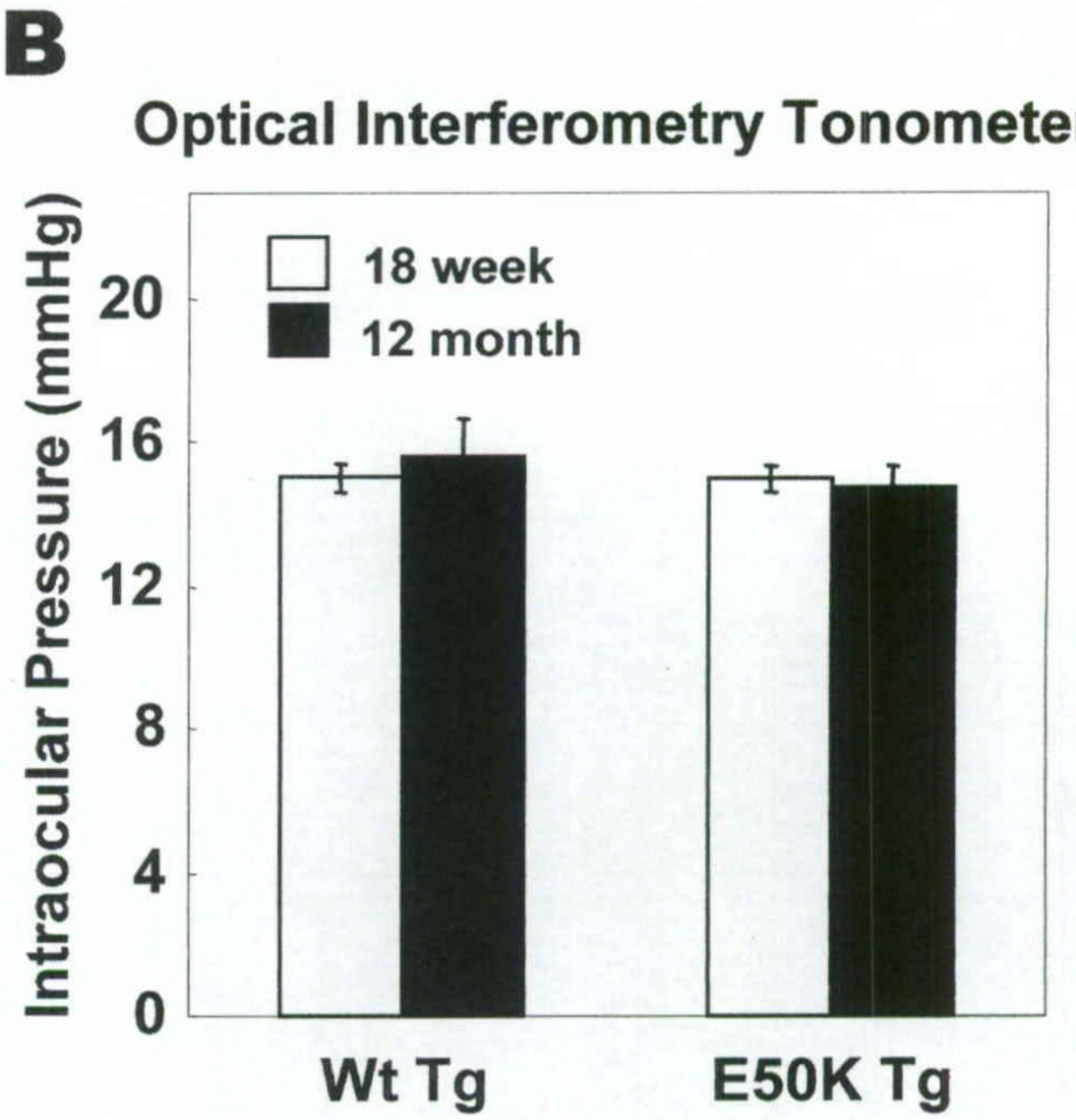
B
Optical Interferometry Tonometer
18 week
12 month
Intraocular Pressure (mmHg)
0
4
8
12
16
20
Wt Tg
E50K Tg

A

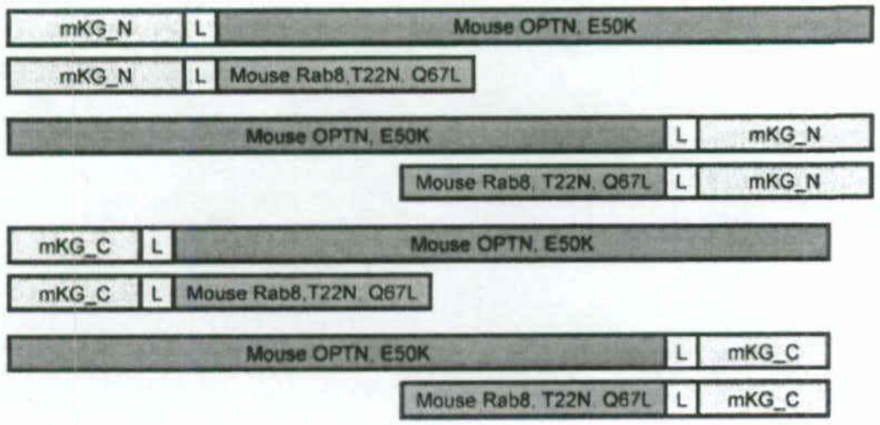
mKG_N
L
Mouse OPTN, E50K
mKG_N
L
Mouse Rab8,T22N, Q67L
Mouse OPTN, E50K
L
mKG_N
Mouse Rab8, T22N, Q67L
L
mKG_N
mKG_C
L
Mouse OPTN, E50K
mKG_C
L
Mouse Rab8,T22N, Q67L
Mouse OPTN, E50K
L
mKG_C
Mouse Rab8, T22N, Q67L
L
mKG_C

B

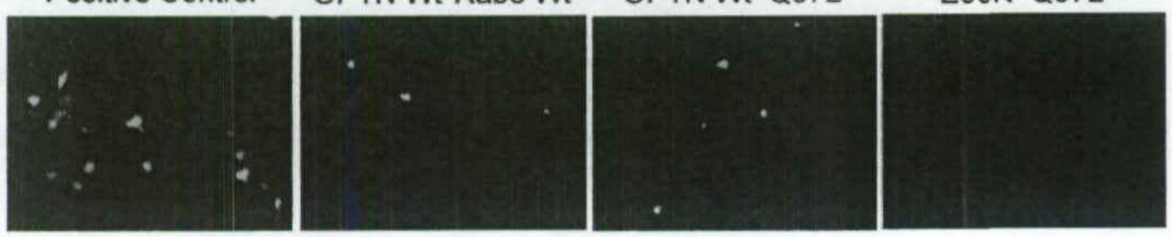
Positive Control
OPTN Wt-Rab8 Wt
OPTN Wt-Q67L
E50K-Q67L

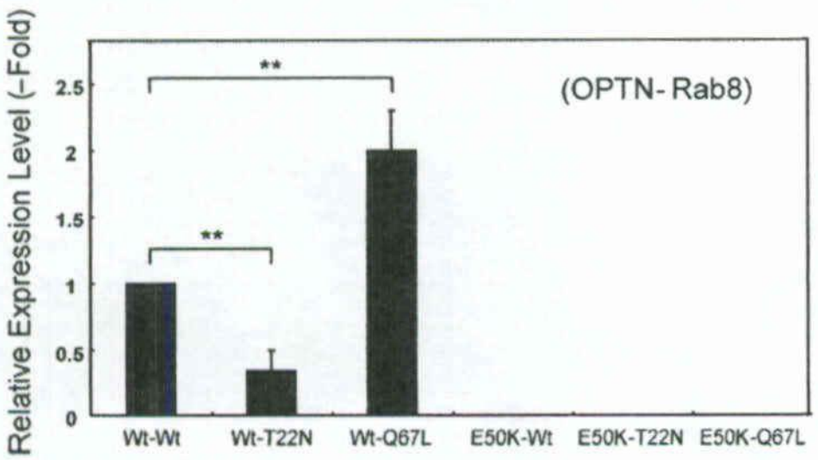
Relative Expression Level (-Fold)
2.5
2
1.5
1
0.5
0
**
**
(OPTN- Rab8)
Wt-Wt
Wt-T22N
Wt-Q67L
E50K-Wt
E50K-T22N
E50K-Q67L

C

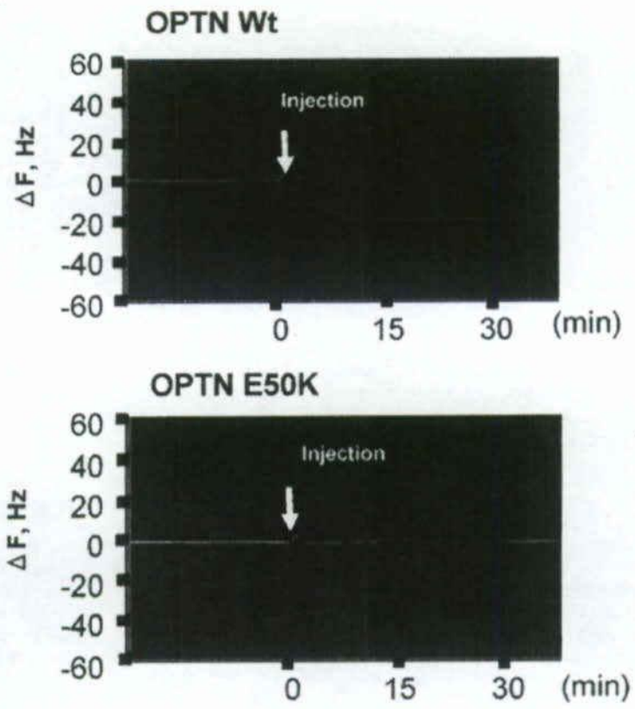
OPTN Wt
ΔF, Hz
60
40
20
0
-20
-40
-60
Injection
0
15
30
(min)
OPTN E50K
ΔF, Hz
60
40
20
0
-20
-40
-60
Injection
0
15
30
(min)

D

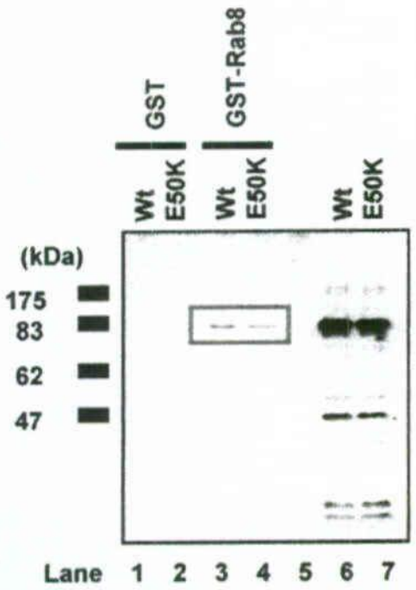
GST
GST-Rab8
Wt
E50K
Wt
E50K
Wt
E50K
(kDa)
175
83
62
47
Lane 1 2 3 4 5 6 7

E

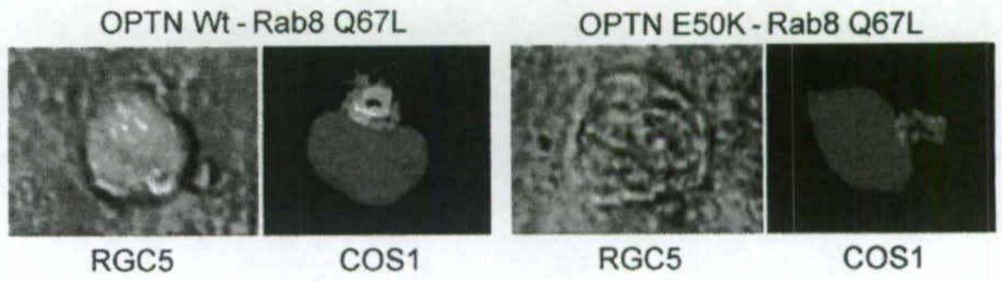
OPTN Wt - Rab8 Q67L
OPTN E50K - Rab8 Q67L
RGC5
COS1
RGC5
COS1

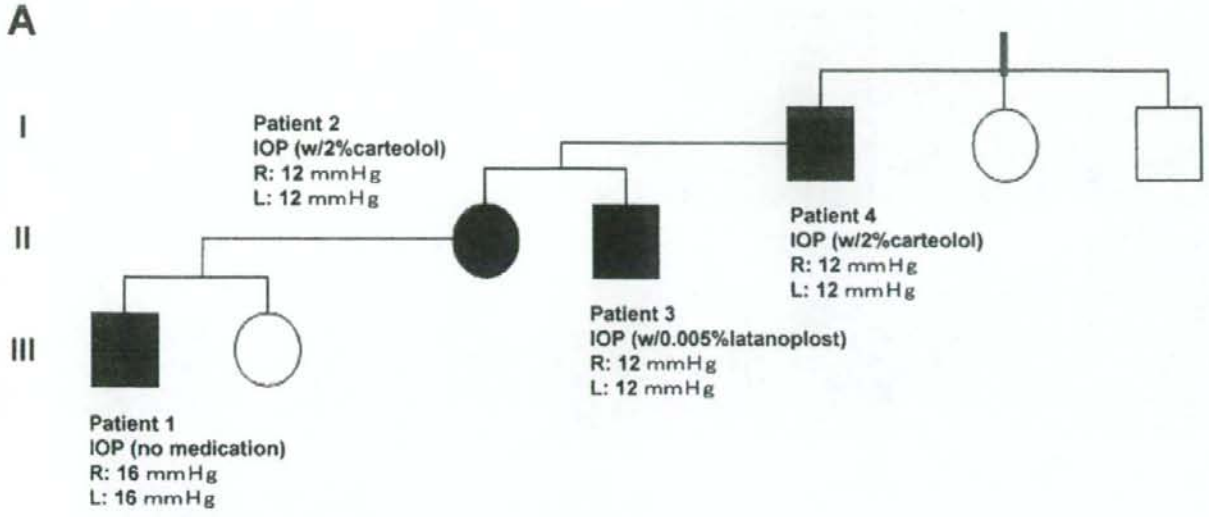
A
I
II
III
Patient 2
IOP (w/2%carteolol)
R: 12 mmHg
L: 12 mmHg
Patient 4
IOP (w/2%carteolol)
R: 12 mmHg
L: 12 mmHg
Patient 3
IOP (w/0.005%latanoplost)
R: 12 mmHg
L: 12 mmHg
Patient 1
IOP (no medication)
R: 16 mmHg
L: 16 mmHg

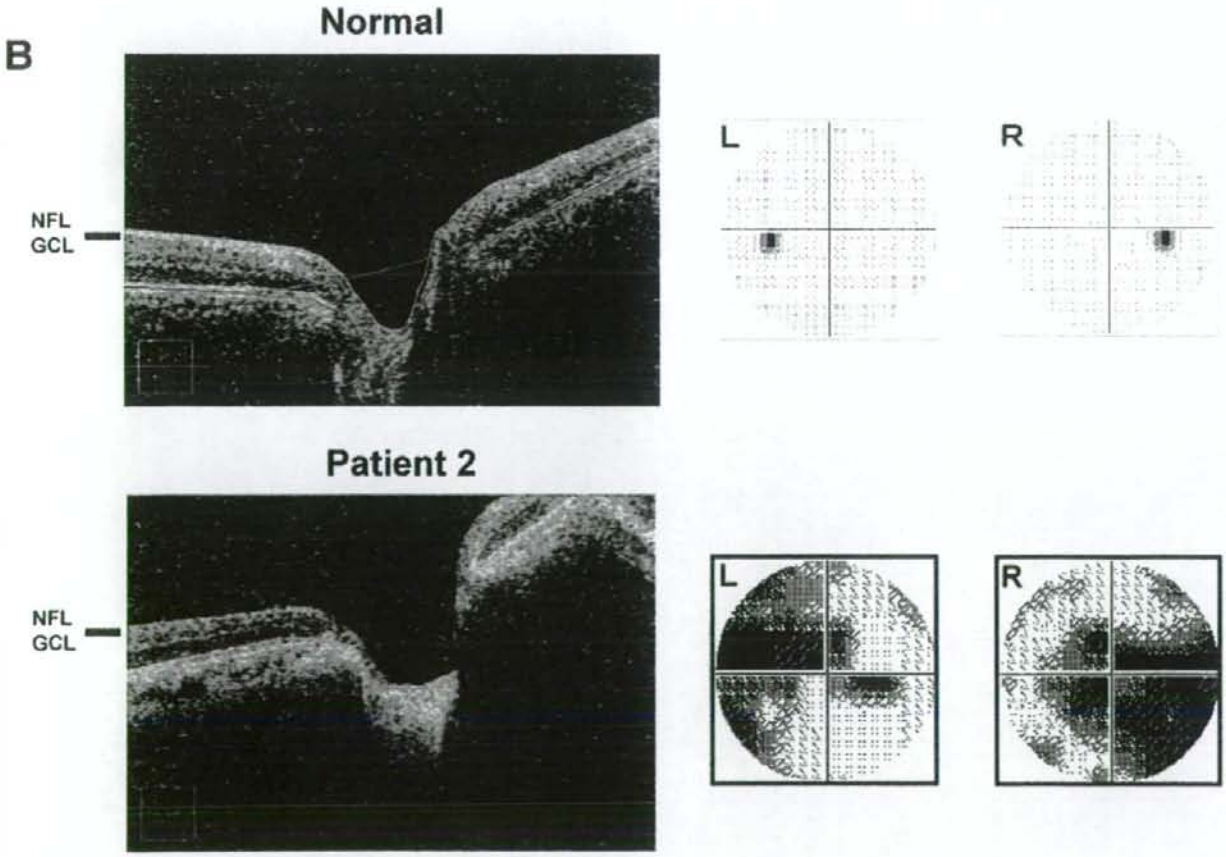
B
Normal
NFL
GCL
L
R
Patient 2
NFL
GCL
L
R

High Resolution Genome-wide Association Study on Advanced Wet-type Age-Related Macular Degeneration

Asako Seki[1*], Masakazu Akahori[1*], Haru Okamoto[1], Masayoshi Minami[1], Naoki Terauchi[2], Minoru Obazawa[2], Tohru Noda[2], Miki Honda[3], Atsushi Mizota[3], Minoru Tanaka[3], Takeshi Iwata[1]

*These two authors contributed equally to this manuscript

[1]National Institute of Sensory Organs, National Hospital Organization Tokyo Medical Center, Meguro-ku, Tokyo, Japan. [2]Division of Ophthalmology, National Hospital Organization Tokyo Medical Center, Meguro-ku, Tokyo, Japan. [3]Department of Ophthalmology, Juntendo University Urayasu Hospital, Urayasu, Chiba, Japan.

Correspondence to: Takeshi Iwata, Ph.D.

Division of Molecular & Cellular Biology, National Institute of Sensory Organs, National Hospital Organization Tokyo Medical Center, 2-5-1 Higashigaoka, Meguro-ku, Tokyo 152-8902 Japan.

TEL/FAX: +81-3-34111026

Email: iwatatakeshi@kankakuki.go.jp

Word count: